GEOPHYSICAL RESEARCH LETTERS, VOL. 27, NO. 2, PAGES 165-168, JANUARY 15, 2000

Simultaneous triggered VLF emissions and energetic electron distributions observed on POLAR with PWI and HYDRA

T. F. Bell, U. S. Inan, and R. A. Helliwell
STAR Laboratory, Stanford University, Stanford, CA

J. D. Scudder
Department of Physics and Astronomy, University of Iowa, Iowa City, IA

Abstract. We report simultaneous observations of energetic 1-20 keV electrons and VLF emissions triggered within the plasmasphere by pulses from ground based VLF transmitters, using the PWI and HYDRA instruments on the POLAR spacecraft. The 1-20 keV electrons have the correct energy to interact with the input pulses through gyoresonance. Emissions are generated by the pulses only when the particle flux is enhanced well above background and the particle pitch angle distribution is very highly anisotropic, with the average equatorial pitch angle exceeding $\sim$ 75°. Because of these high pitch angles, the particles are trapped typically within 7° of the magnetic equator. Only pulses which propagate within whistler mode ducts are observed to trigger emissions. The observed pitch angle anisoptropies are much larger than those assumed in present models of the VLF emission triggering phenomenon, and thus our observations provide a new starting point for understanding the emission process.

1. Introduction

Within the plasmasphere, discrete VLF emissions are commonly triggered by externally generated discrete whistler mode waves such as lightning generated whistlers and signals from ground based VLF transmitters, with peak emission intensities reaching values as large as 16 pT [*Bell, 1985*]. The triggered emissions are thought to be generated near the magnetic equator through a gyroresonance interaction between $\sim$ 1-20 keV energetic electrons and the triggering wave in which the particle pitch angles are altered and free energy is transferred from the particles to the waves [*Helliwell, 1967; Matsumoto and Kimura, 1971; Omura, et al., 1991; Nunn and Smith 1996*]. Understanding the emission process is important since these interactions can directly affect the lifetimes of the resonant electrons.

Few observations have been made of the plasmaspheric energetic electron population in the 1 to 20 keV energy range near the magnetic equator. *Shield and Frank* [*1970*] provided only a small data set with crude pitch angle resolution, while Explorer 45 observations [*Lyons and Williams, 1975*] concerned electron energies of 35 keV and above. Subsequent magnetospheric missions such as ISEE-1 and DE-1 acquired very little plasmaspheric particle data in the 1-20 keV energy range. Thus the HYDRA data presented here represents the first detailed pitch angle and energy measurements of plasmaspheric electrons in the 1-20 keV energy range.

The triggered emission process can be studied most simply by focusing on the emissions triggered by signals from known sources such as ground-based VLF transmitters [*Bell et al, 1981; Bell, 1985*]. In the present work we present simultaneous plasma wave and energetic electron data acquired with the PWI and HYDRA instruments on the POLAR spacecraft during periods when VLF emissions were triggered by VLF transmitter signals. In all cases the velocity distribution of the resonant electrons is highly anisotropic, with the average electron equatorial pitch angle exceeding $\sim$ 75°.

2. Observations

We report data acquired during six periods in 1996 and 1997 when the Plasma Wave Instrument (PWI) [*Gurnett et al., 1995*] observed VLF emission triggering as the POLAR spacecraft moved within the plasmasphere near the magnetic equatorial plane. We concentrate on the period 0445-0550 UT, 13 Jan 1997, since the data from this period is typical of the entire data set. Figure 1 shows a frequency-time spectrogram of PWI data acquired near the magnetic equator at L=3.3 during the period when VLF emissions were being triggered by fixed frequency signals from an Omega VLF navigation transmitter in Aldra, Norway. The upper panel shows the overall plasma wave activity over the 0-12.5 kHz frequency range. There is evidence of wave generation in the form of hiss in the frequency bands 0-2 and 4-6 kHz. However above 7 kHz there are no prominent natural waves other than those triggered by the Omega pulses. The lower panel shows a smaller frequency range which includes fixed frequency pulses from the Omega transmitter as well as VLF emissions excited by the pulses. The pulses consist of a set of three. Utilizing the measured time delays of the Omega pulses in conjunction with ray tracing calculations, it is found that the first ariving pulse in each set propagates directly to POLAR from the ground along a non-ducted ray path [*Bell et al, 1981*]. The second and third pulses occur because some of the wave energy from the transmitter enters a duct in the northern hemisphere and propagates to the conjugate hemisphere within the duct, and

Paper number 1999GL003673.
0094-8276/00/1999GL003673$05.00

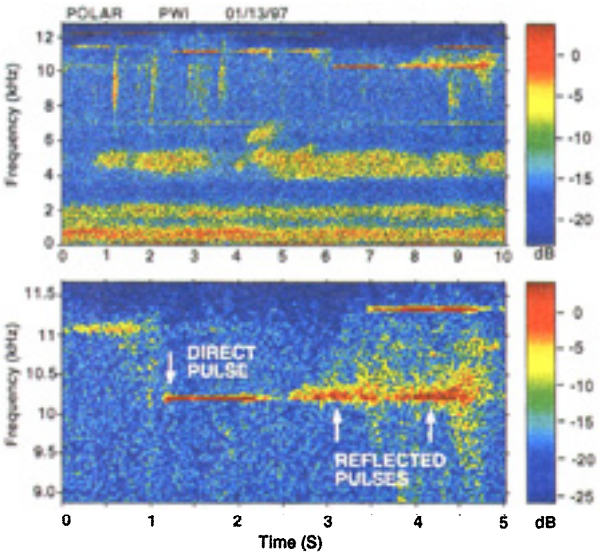

Figure 1. Typical frequency-time spectrograms of PWI data showing VLF emission triggering events.

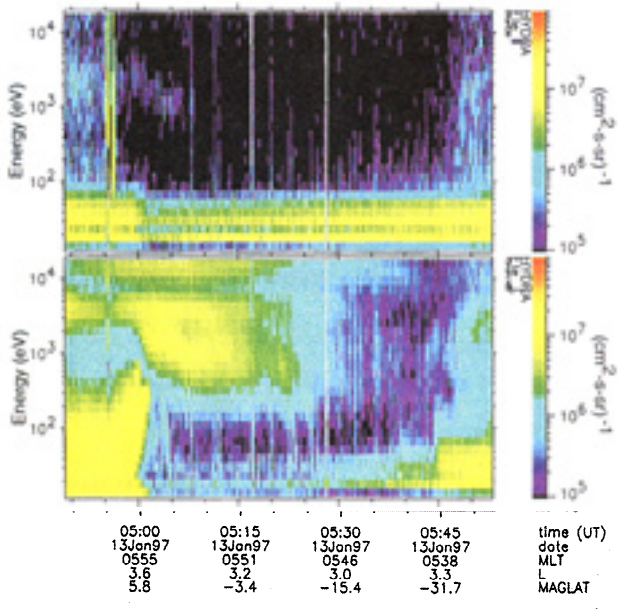

Figure 3. Differential energy flux-time spectrograms showing HYDRA 0-20 keV electron data during a period of VLF emission triggering.

during the reflection process at the duct end point in the south, some of the wave energy is back scattered along a non-ducted path to POLAR. This backscattered component produces the second pulse. The ducted signal then propagates back to the northern hemisphere where additional wave energy is reflected and scattered back to POLAR, producing the third pulse, as illustrated in Figure 2. This hybrid mode of propagation has been frequently observed in the past [*Rastani et al., 1985*]. Only the signals which have propagated within the duct excite VLF emissions. From the time delays of the direct and backscattered Omega pulses and the plasma density measurements from PWI, the L shell of the duct can be estimated as $L = 3.4 \pm 0.1$.

HYDRA [*Scudder at al., 1995*] plasmaspheric observations of energetic electrons during the emission events are shown as the flux-time spectrograms of Figure 3. The lower panel shows $j_\perp$, the differential energy flux for electrons with pitch angle α in the range $75° \leq \alpha \leq 105°$, i.e., $\sim$ perpendicular to the ambient vector magnetic field B_o. The upper panel shows $j_\parallel$, the differential energy flux for electrons with $\alpha \leq 30°$, i.e., $\sim$ parallel to B_o. POLAR entered the plasmaphere at $\sim$ 0500 UT and exited the plasmasphere at $\sim$ 0545 UT, according to plasma density measurements by the PWI Sweep Frequency Receiver. The magnetic equator is crossed at $\sim$ 0510 UT at L $\sim$ 3.3.

Within the plasmasphere, $j_\perp$ is initially large, while $j_\parallel$ is near the background level. As POLAR moves south from the magnetic equator, staying roughly tangent to the L $\sim$ 3.2 magnetic field line, $j_\perp$ decreases rapidly and at a geomagnetic latitude of $-15°$, has decreased by $\sim$ a factor of 10 from its equatorial value. This large variation cannot be due to L shell dependence, because POLAR samples each L shell twice, and only the low latitude intersections show such high fluxes. Thus the HYDRA observations indicate that the population of 1-20 keV energetic electrons is localized to the near vicinity of the magnetic equator and that the pitch angle distribution of these electrons is highly anisotropic. A similar distribution has recently been proposed to explain ground based observations of triggered VLF emissions [*Sonwalkar et al.,1997*].

Figure 4 shows $j_\perp$ and $j_\parallel$ at 20 keV energy at the magnetic equatorial plane for all POLAR orbits for January 1997, except one for which no data was available. The local time of the equatorial crossing was either $\sim$ 0600 UT or $\sim$ 1800 LT, and the L shell ranged from 2.8 - 3.5. The crossings are shown in sequence. The top panel concerns the 0600 LT crossings; the bottom panel, the 1800 LT crossings. At both local times $j_\perp$ exceeds $j_\parallel$ by at least a factor of 5, and the average ratio is $\sim$ 14. Since the loss cone angle at L $\sim$ 3 is $\sim 8°$, which is small compared to the 30° range sampled by the parallel detectors, an absence of particles within the loss cone cannot explain these large ratios. Similar results are obtained for other electron energies in the 1-20 keV range, implying that the large pitch angle anisotropies deduced from Figure 3 are a common feature of 1-20 keV electrons in the plasmasphere.

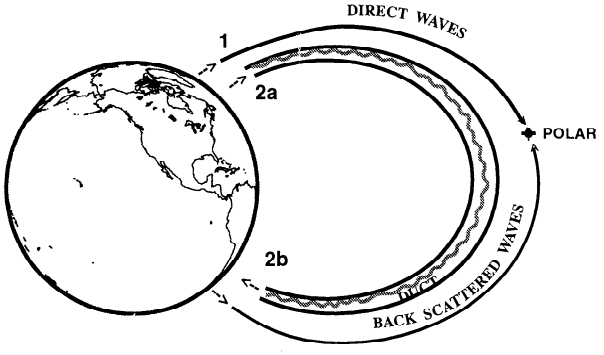

Figure 2. Schematic of Omega pulse propagation modes to POLAR.

3. Interpretation

As a result of the large pitch angle anisotropy of the 1-20 keV plasmaspheric electrons, VLF whistler mode

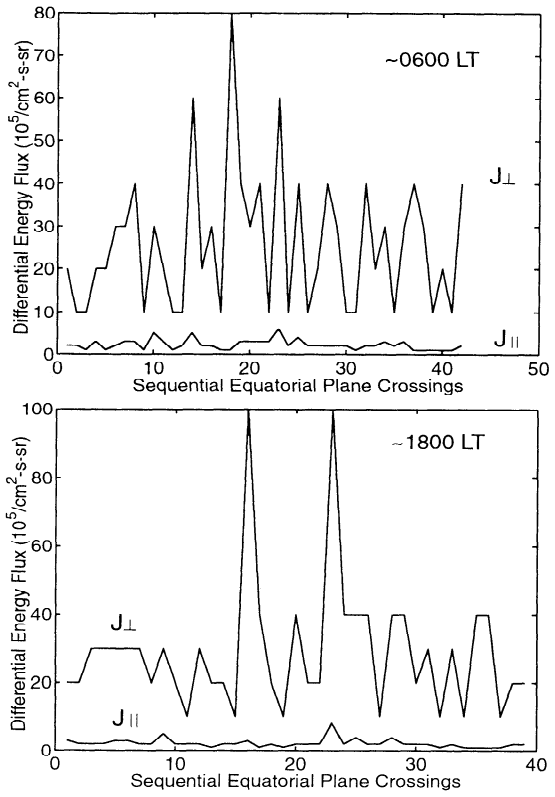

Figure 4. Plots showing the differential energy flux at 20 keV for both the perpendicular ($j_\perp$) and parallel ($j_\parallel$) directions at the magnetic equator during Jan 1997.

waves in gyroresonance with these electrons may be amplified through the whistler mode cyclotron instability [*Bell and Buneman, 1964; Helliwell, 1967; Matsumoto and Kimura, 1971*]. The well known resonance condition for this instability is : $v_\parallel = (\omega - \omega_H)/k_\parallel$, where $v_\parallel$ is the electron velocity parallel to B_o, ω_H is the electron gyrofrequency, ω is the wave frequency, and $k_\parallel$ is the component of the wave number parallel to B_o.

For a magnetized plasma with a small population of energetic electrons in the presence of a larger population of cold electrons, the linear temporal growth rate of the cyclotron instability for a plane wave varying as $e^{i(\omega t - kz)}$ is [*Matsumoto and Kimura, 1971*]:

$$\omega_i = \frac{-\pi}{2N_h}\frac{\omega_H \omega_{oh}^2}{\partial D/\partial \omega_r}\int v_\perp \delta(\omega_r - kv_\parallel - \omega_H)\nabla_v f_h d\vec{v} \quad (1)$$

where ω_r and ω_i are respectively the real and the imaginary part of ω, N_h is the total number density of the energetic electrons, ω_{oh} is the plasma frequency associated with the energetic electrons, $v_\perp$ is the energetic electron velocity perpendicular to B_o, f_h is the distribution function of the energetic electrons $\delta(-)$ is the Dirac delta function, $D = c^2k^2 - w_r^2 + \frac{\omega_r \omega_o^2}{\omega_r - \omega_H}$ is the dispersion relation for the whistler mode waves, ω_o is the plasma frequency of the cold plasma electrons, and the operator ∇_v is defined as $\nabla_v = \frac{\partial}{\partial v_\perp} - \frac{kv_\perp}{\omega_H}\frac{\partial}{\partial v_\parallel}$.

The linear temporal growth rate given in (1) is equivalent to a spatial growth rate $k_i = \omega_i/v_g$, where v_g is the group velocity of the wave. Thus the total wave amplification in dB over a distance z along B_o is:

$$G = 20\log_{10}[e^{\int k_i dz}] = 8.7\int k_i dz. \quad (2)$$

To evaluate (2) we need to determine $f_h(\vec{v}, z)$, or equivalently $f_h(\vec{v}, \lambda)$, where λ is the magnetic latitude. We note from Liouvilles' theorem that $f_h(\vec{v}, \lambda)$ is constant along the particle trajectories in phase space. Thus at any latitude λ we can write $f_h(v, \alpha, \lambda) = f_{he}(v_e, \alpha_e, \lambda = 0)$ where f_{he} is the distribution at the magnetic equator and v_e and α_e are the values of particle velocity and pitch angle there. But from conservation of energy and magnetic moment we have $v_e = v$ and:

$$\alpha_e(\lambda, \alpha) = \sin^{-1}\left[\sqrt{\frac{B_{oe}}{|B_o(\lambda)|}}\sin\alpha\right] \quad (3)$$

where $B_{oe} = |B_o(\lambda = 0)|$ = magnitude of B_o at the magnetic equator. Thus $f_h(v, \alpha, \lambda) = f_{he}(v, \alpha_e(\lambda, \alpha))$. Since at any latitude λ, $j_\perp(\lambda) = \frac{1}{2}f_h(v, \frac{\pi}{2}, \lambda)v^4 = \frac{1}{2}f_{he}(v, \alpha_e(\lambda, \frac{\pi}{2}))v^4$, we can find the complete form of $f_{he}(v, \alpha_e)$ if $j_\perp(\lambda)$ is known.

Assuming that f_{he} does not change markedly between L= 3.0-3.2, we can apply the above relations to the data of Figure 3 to find to first order:

$$f_h(v, \alpha, \lambda) = 1.6 \times 10^7\left[\sqrt{\frac{B_{oe}}{|B_o(\lambda)|}}sin\alpha\right]^\gamma v^{-4} \quad (4)$$

where $\gamma \sim 25$. Equations (1), (2), and (4) were used to determine the total amplification of a ducted VLF whistler mode wave crossing the magnetic equator within the plasmasphere. The results are shown in Figure 5 for a 10.2 kHz wave on various L shells. Two curves are shown in the Figure. The solid curve represents the amplification due to the 1-20 keV fluxes observed by HYDRA and modeled by (4). The dashed curve represents the amplification that would be expected if (4) were extrapolated to 50 keV. Extrapolation is necessary here because data from the POLAR IES instrument [*Blake et al., 1995*], which measures the flux and pitch angle of energetic electrons above 18.5 keV, was contaminated by intense energetic proton fluxes whenever POLAR was within the plasmasphere. Consequently we do not know the characteristics of the energetic electron flux above 20 keV. In terms of velocity dependence the extrapolation appears reasonable since Explorer 45 observations [*Lyons and Williams, 1975*] show post

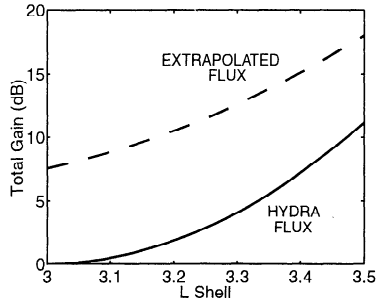

Figure 5. Plot of total linear amplification as a function of L shell for VLF waves propagating in a duct across the magnetic equator.

storm perpendicular differential number fluxes of $\sim 10^5(cm^2 - s - sr - keV)^{-1}$ at L $\sim$ 3 for electron energies in the 35-70 keV range. Taking the midrange energy of $\sim$ 50 keV, the corresponding differential energy flux would be $\sim 5 \times 10^6(cm^2 - s - sr)^{-1}$ which is very close to the value shown for 20 keV in Figure 3. Thus the assumption of $j_\perp \sim$ *constant* appears reasonable up to $\sim$ 50 keV. On the other hand the pitch angle anisotropy of the Explorer 45 differential number flux for 35-70 keV was much less than that displayed in the HYDRA data for the 1-20 keV electrons. Thus the assumption that $f_h \sim [sin\alpha]^{25}$ for energies between 20 and 50 keV may be a poor one. Nevertheless the total gain of the whistler mode wave is not a strong function of γ, as long as $\gamma \geq 4$.

4. Discussion

VLF emissions are believed to be generated through a nonlinear phase trapping mechanism inherent to the cyclotron resonance interaction [*Helliwell,1967; Carlson et al., 1990; Omura et al., 1991; Bell, 1964; 1984*]. For any given resonant electron, nonlinear phase trapping becomes important only after a time $\Delta t_p \sim {\omega_t}^{-1}$, where $\omega_t = [\eta B_w k v_\perp]^{\frac{1}{2}}$ is the nonlinear phase trapping frequency, η is the electron charge-to-mass ratio and B_w is the magnetic field amplitude of the whistler mode wave. The resonance can endure for the time Δt_p only if during this time ${\omega_t}^2 \geq h(z)$, where $h(z)$ is a function of the local mirror force and local gradients in B_o and ω_o, as defined in [*Bell, 1984*]. For electrons with high pitch angles, the mirror force dominates, and $h(z) \sim k\mu\frac{\partial\omega_H}{\partial z}$, where μ is the electon magnetic moment.

Most recent models of the nonlinear phase trapping mechanism [*eg, Carlson et al., 1990; Omura et al., 1991; Nunn and Smith, 1996*] include the effects of the mirror force on the resonant electrons, but have not considered energetic electron populations with pitch angle anisotropies as large as those observed on POLAR. One effect of this anisotropy is that most of the energetic electrons mirror very close to the magnetic equatorial plane. For example the average pitch angle of the distribution given in (4) is $< \alpha_e > = 81°$, and the average particle at each energy will mirror at $\lambda \sim \pm 4°$ in a dipole model of B_o. It can be shown that the mirror force at this latitude at L = 3.5 is sufficiently strong that the condition ${\omega_t}^2 \geq h(z)$ for gyroresonant 20 keV electrons requires $B_w \geq 10$ pT, a value $\sim$ 40 dB above the Omega signal input levels measured by PWI and 20 dB more than that shown in Figure 5. Thus the mirror force becomes the dominant factor in limiting the nonlinear phase bunching mechanism. Because of this feature, as well as the unexpected nature of the electron distribution, the data presented here represents a new starting point for models of VLF emission generation within the plasmasphere.

Acknowledgments. Stanford workers were supported by subcontract with the University of Iowa under NASA/GSFC grant NAS5-30371. J. Scudder was supported through NASA grant NAG 5-2834. We thank J. Yarbrough for preparing the PWI spectrograms.

References

Bell, T. F. and O. Buneman, Plasma instability in the whistler mode caused by a gyrating electron stream, *Phys. Rev., 133*, A1300, 1964.

Bell, T. F., U. S. Inan, and R. A. Helliwell, Nonducted coherent VLF waves and associated triggered emissions observed on the ISEE-1 satellite, *J. Geophys. Res., 86*, 4649, 1981.

Bell, T. F., The nonlinear gyroresonance interaction between energetic electrons and coherent VLF waves propogating at an arbitrary angle with respect to the Earth's magnetic field, *J. Geophys. Res., 89*, 905, 1984.

Bell, T.F., High amplitude VLF transmitter signals and associated sidebands observed near the magnetic equatorial plane on the ISEE 1 satellite, *J. Geophys. Res., 90*, 2792, 1985.

Blake, J. B., et al., CEPPAD, pages 531-562, *The Global Geospace Mission* , C. T. Russell (ed.), Kluwer Academic Publishers, London, 1995.

Carlson, C. R., R. A. Helliwell, and U. S. Inan, Space-time evolution of whistler mode wave growth in the magnetosphere, *J. Geophys. Res., 95*, 15,073, 1990.

Gurnett, D. A., et al., The polar plasma wave instrument, pages 597-622, *The Global Geospace Mission* , C. T. Russell (ed.), Kluwer Academic Publishers, London, 1995.

Helliwell, R. A., A theory of discrete emissions from the magnetosphere, *J. Geophys. Res., 72*, 4773, 1967.

Lyons, L. R., and D. J. Williams, The storm and post storm evolution of energetic (35-560 keV) radiation belt electron distributions, *J. Geophys. Res., 80*, 3985, 1975.

Matsumoto, H., and I. Kimura, Linear and nonlinear cyclotron instability and VLF emissions in the magnetosphere, *Planet. Space. Sci., 19*, 567, 1971.

Nunn, D., and A. J. Smith, Numerical simulation of whistler-triggered VLF emissions observed in Antarctica, *J. Geophys. Res., 101*, 5261, 1996.

Omura, Y., D. Nunn, H. Matsumoto, and M. J. Rycroft, A review of observational, theoretical and nemerical studies of VLF triggered emissions, *J. Atmos. Terr. Phys., 53*, 351, 1991.

Rastani, K., U. S. Inan, and R. A. Helliwell, DE 1 observations of Siple transmitter signals and associated sidebands, *J. Geophys. Res., 90*, 4128, 1985

Schield, M. A., and L. A. Frank, Electron observations between the inner edge of the plasma sheet and the plasmasphere, *J. Geophys. Res., 75*, 5401, 1970.

Scudder, J., et al., Hydra - A 3-Dimensional Electron and Ion Hot Plasma Instrument for the Polar Spacecraft of the GGS Mission, pages 459-495, *The Global Geospace Mission* , C. T. Russell (ed.), Kluwer Academic Publishers, London,1995.

Sonwalkar, V. S., et al., Properties of the magnetospheric hot plasma deduced from whistler mode wave injection at 2400 Hz: Ground-based detection of azimuthal structure in magnetospheric hot plasmas, *J. Geophys. Res., 102*, 14363, 1997

T. Bell, U. Inan, and R. Helliwell, STAR Laboratory, Stanford University, Stanford, CA. 94305 (e-mail: bell@nova.stanford.edu)

J. Scudder, Dept. of Phys. and Astr., University of Iowa, Iowa City, IA 52242

(Received September 14, 1999; accepted October 27, 1999.)